

# Observation of large atomic-recoil-induced asymmetries in cold atom spectroscopy

C. W. Oates, G. Wilpers, and L. Hollberg

Time and Frequency Division, National Institute of Standards and Technology, 325 Broadway, Boulder, Colorado 80305, USA

(Received 12 November 2003; published 10 February 2005)

The atomic-recoil effect leads to large (25%) asymmetries in a nearly ideal form of saturation spectroscopy based on Ca atoms that have been laser-cooled to 10  $\mu\text{K}$ . Starting with spectra from the more familiar Doppler-broadened domain, we show how the fundamental asymmetry between absorption and stimulated emission of light manifests itself when shorter spectroscopic pulses lead to the Fourier transform regime. These effects occur on frequency scales much larger than the size of the recoil shift itself, and have not been described before in saturation spectroscopy. These results directly impact precision spectroscopic measurements.

DOI: 10.1103/PhysRevA.71.023404

PACS number(s): 32.80.-t, 42.62.Fi

## I. INTRODUCTION

The effects of atomic recoil have been of considerable interest to laser spectroscopists for more than 30 years [1] and are the foundation of laser cooling of atoms. The first experimental evidence that saturation absorption spectroscopy produced a recoil splitting in the Doppler-free spectra of atomic and molecular lines was demonstrated by Hall, Bordé, and Uehara using a high-resolution laser spectrometer [2]. Since then there have been several beautiful demonstrations of recoil splitting via various forms of saturation spectroscopy (see, for example, Refs. [3–6]). In all of these studies the closely spaced recoil components were superimposed on a broad Doppler background, thereby obscuring the recoil-induced asymmetries inherent in light-atom interactions.

In the work presented here, we use a nearly ideal saturation spectroscopic configuration to show how the small effect of atomic recoil can cause large asymmetries in the spectra of samples of freely expanding microkelvin atoms. At sub-recoil resolutions, we take advantage of the narrow width of the Doppler background (only seven times that of the recoil splitting) to clearly expose the asymmetry of the recoil components. Moreover, by gradually reducing the resolution, we show how the recoil effect leads to large spectral asymmetries in the Fourier-transform limit (see Fig. 1), which is a relevant regime for many precision spectroscopy experiments. Surprisingly, these effects can appear on a frequency scale more than ten times larger than the size of the recoil effect itself. We emphasize that these recoil effects are fundamentally different from asymmetries described in earlier papers, which resulted from spontaneous emission or collisional quenching [1,2]. Not only is this asymmetry of interest from the point of view of basic physics, it also has important implications for future optical clocks based on laser-cooled neutral atoms [7,8].

## II. RECOIL SPLITTING IN SATURATION SPECTROSCOPY

As described elsewhere, the recoil doublet can be readily understood from conservation of momentum and energy [1,2]. When an atom initially at rest absorbs a photon of frequency  $\nu$ , it recoils with a velocity,  $v_r = h\nu/mc$ , where  $m$  is

the atomic mass,  $h$  is Planck's constant, and  $c$  is the speed of light. For a two-level atom with an energy level spacing of  $E_0 = h\nu_0$ , this absorption resonance occurs at a frequency,

$$\nu_A = \nu_0 + \frac{1}{2} \frac{h\nu_0^2}{mc^2} = \nu_0 + \frac{1}{2} \nu_r. \quad (1)$$

Equation (1) shows that the incident photon needs to supply energy for both the internal and external degrees of freedom (i.e., atomic excitation and recoil). For an atom at rest but starting in the excited state, a similar analysis shows that the resonance for stimulated emission occurs at a frequency

$$\nu_{SE} = \nu_0 - \frac{1}{2} \frac{h\nu_0^2}{mc^2} = \nu_0 - \frac{1}{2} \nu_r. \quad (2)$$

In this case the energy of the internal degree of freedom ( $h\nu_0$ ) must supply the energy for both the emitted photon and the recoil kick. Thus the stimulated emission resonance is red-shifted relative to that for absorption by  $\nu_r$ , the splitting of the recoil doublet, which is typically tens of kilohertz for

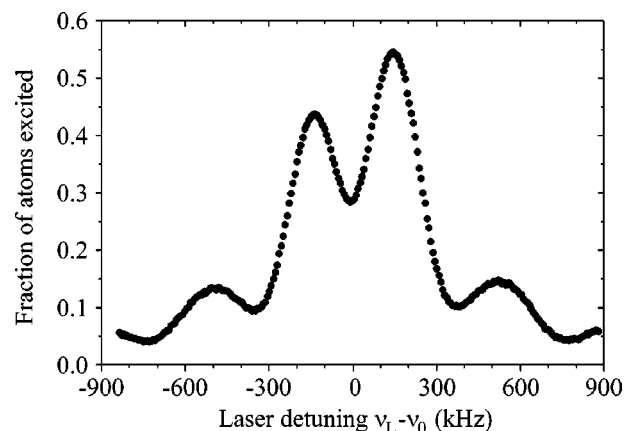


FIG. 1. Two-pulse saturated absorption spectrum as a function of laser detuning from the Bohr frequency with a probe pulse duration of 2.6  $\mu\text{s}$  (corresponding to a resolution of 320 kHz). Due to the narrow velocity distribution, this spectrum is Fourier-transform limited, and shows a large asymmetry resulting from recoil effects. Even though the recoil splitting of 23.1 kHz is unresolved, the recoil-induced asymmetry is apparent over a range of  $>500$  kHz.

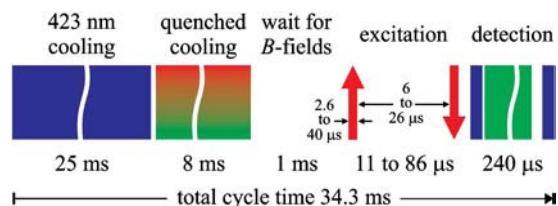


FIG. 2. Experimental sequence for a single measurement. The atoms are cooled first to 2 mK with cooling on the 423 nm transition and then further cooled to 10  $\mu$ K with quenched narrow line cooling on the 657 nm transition. With the trap turned off and the magnetic fields settled, the atoms are excited with a pair of counterpropagating  $\pi$  pulses separated in time, after which the fraction of atoms excited is measured using a normalization scheme.

optical transitions in low mass atoms. This frequency splitting ensures that the alternating absorption and stimulated emission cycles in Rabi flopping are simultaneously resonant even when the Doppler shift associated with the atomic recoil is included. Thus the recoil splitting is not readily observed with a laser beam from a single direction. Instead, one can use two counterpropagating laser beams, the usual configuration for saturation spectroscopy. Then the atomic recoil due to photon absorption from one beam pushes an atom toward the counterpropagating beam, effectively reversing the sign of the recoil shift. In this way it is possible to see two distinct sub-Doppler features split by  $\nu_r$ , although this small splitting can only be resolved in ultrahigh-resolution experiments.

### III. EXPERIMENTAL APPARATUS

In this investigation, we take advantage of the capabilities of our optical clock apparatus [7] to perform a nearly ideal form of saturation spectroscopy. We excite a laser-cooled (temperature = 10  $\mu$ K) sample of neutral Ca atoms using the closed 657 nm clock transition between the  $^1S_0$  ground state and the metastable  $^3P_1$  excited state (lifetime of 340  $\mu$ s). To avoid multiphoton processes and keep the interpretation as simple as possible, we excite the atoms sequentially with single  $\pi$  pulses (i.e., ones that yield unit excitation on resonance) at the same laser frequency from two opposing directions. Sequential excitation greatly simplifies the analysis, since it removes the possibility of events containing more than one photon from each direction that can distort the line shape [2,3,9]. With transit-time broadening and spontaneous emission negligible, we can change the spectroscopic resolution just by changing the duration of the square probe pulses. We realize these experimental conditions with the following measurement cycle (see Fig. 2) [7]. First, we load atoms from a Ca beam into a magneto-optic trap using the strongly-allowed 423 nm cooling transition. We then turn off the 423 nm light and use a 3-dimensional quenched narrow-line cooling scheme based on the clock transition to reduce the temperature of the atomic sample ( $\sim 10^6$  atoms) to about 10  $\mu$ K [7,10]. When the atoms are cold, we switch off the trap and turn on a magnetic bias field ( $>200$   $\mu$ T) to perform the spectroscopy on the narrow  $m=0 \rightarrow m=0$  clock transition.

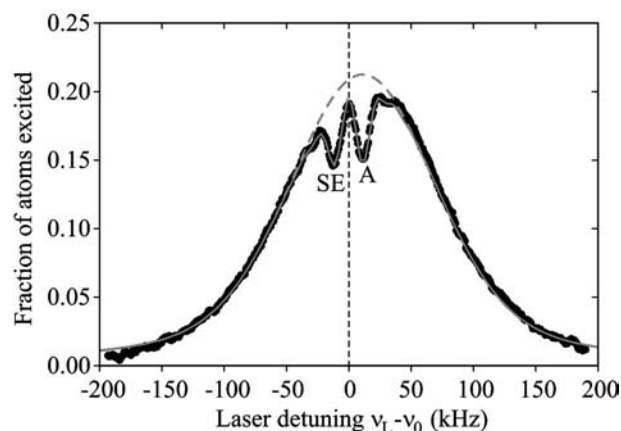


FIG. 3. Two-pulse saturated absorption spectrum (circles) as a function of laser detuning from the Bohr frequency with a probe pulse duration of 40  $\mu$ s (21 kHz resolution). Clearly seen are the saturation dips separated by the recoil splitting superimposed on the Doppler background, with the stimulated emission component (“SE”) red-shifted and the absorption component (“A”) centered. Shown for comparison is a simulated Doppler curve doubled in height (dashed line). Note that the much smaller features on the outside wings of the dips result from the  $(\sin x/x)^2$  spectrum of the excitation pulses.

We probe the 657 nm clock transition with pulses derived from a cw diode laser, which is locked tightly to a narrow fringe (9 kHz linewidth) of an environmentally isolated Fabry-Pérot cavity, producing a laser linewidth of less than 5 Hz. Some light from this stabilized master laser is used to injection-lock a slave laser whose output is sent through two acousto-optic modulators to generate the pulses for the opposing directions. The deflected light is steered into optical fibers to spatially filter the beams. The beams coupled out of the fibers expand and are collimated with a diameter of about 6 mm, so that the atoms see flat wave fronts (radius of curvature greater than 50 m). As much as 13 mW can be coupled into these beams, although we adjust the power to produce  $\pi$  pulses. For these measurements we illuminate the atoms with a pulse from one direction, wait 6  $\mu$ s (to make sure the first beam is completely turned off), and then illuminate the atoms with a pulse from the opposite direction. Finally, the fraction of atoms in the excited state is measured using a normalized shelving fluorescence detection technique [7]. We scan the probe frequency ( $\nu_L$ ) slowly (4 s sweep time) while continuously repeating the measurement cycle (duration 34.3 ms, as shown in Fig. 2) to generate our spectra as a function of the laser detuning ( $\nu_L - \nu_0$ ).

### IV. EXPERIMENTAL RESULTS

To make a connection with previous experiments, we first consider the Doppler-broadened regime, for which we choose a pulse duration (40  $\mu$ s) such that the spectroscopic resolution is about 21 kHz. This is considerably less than the 150 kHz (FWHM) Doppler width of the 10  $\mu$ K atoms and slightly less than the 23.1 kHz recoil splitting of the 657 nm clock transition. In Fig. 3 we show the resulting excitation

spectrum, whose envelope is primarily determined by the Doppler background. In fact this envelope has simply twice the height of the curve seen with a single probe pulse, because for most laser frequencies the two counterpropagating laser beams excite nonoverlapping velocity classes on opposite sides of the Doppler distribution.

However, at the absorption resonance frequency,  $\nu_L = \nu_A$  (“A” in Fig. 3), this doubling of the Doppler background is absent, since both beams are resonant with the same velocity group ( $v=0$ ). The first laser pulse has already excited the majority of the atoms in that velocity class to the long-lived excited state. Note that the second pulse cannot deexcite many of these atoms either, since due to atomic recoil they have been shifted out of resonance for stimulated emission. The second resonance (“SE” in Fig. 3), at  $\nu_L = \nu_{SE}$ , results from atoms that started with a velocity  $v = -v_r$ , and were thus excited by the first pulse (in the atoms’ rest frame,  $\nu_L = \nu_A$ ); now at rest in the lab frame due to atomic recoil, they are resonant with the second pulse for stimulated emission, thereby reducing the net fraction of atoms excited.

The two dips resulting from these resonances are analogous to those seen in earlier experiments [2–6,11] but with one important distinction: due to the small width of the Doppler background, we can readily see that the dips are asymmetrically located about the center of the Doppler background. Since the Doppler background results from absorption, it is naturally centered around the resonance at  $\nu_L = \nu_A$ , coincident with the absorption recoil dip. The dip associated with stimulated emission is located one recoil frequency ( $\nu_r$ ) below the absorption resonance, on the red side of the Doppler curve. It is important to emphasize that this asymmetry is not a result of the order of the laser pulses. If we reverse the temporal order, so that the pulse directions are reversed, we observe the identical lineshape, not its mirror image. Rather, this asymmetry is a fundamental feature of saturation spectroscopy, though one that is easily overlooked in experiments with broad Doppler backgrounds. As has been noted by other observers [9,11], this asymmetry can lead to undesired offsets in realizing optical frequency standards based on saturation absorption since the unperturbed line center of the transition (midway between the recoil components) is not centered on the background.

We now consider what happens to this spectrum as the Fourier spectrum of the probe pulse is broadened, not just beyond the recoil splitting but well beyond the width of the Doppler distribution itself. This regime has not previously been investigated experimentally, but is becoming important in state-of-the-art optical atomic clocks based on microkelvin atoms [7,8]. We access this regime by reducing the duration of the probe pulses (while maintaining the pulse area to keep the excitation probability constant). In Fig. 4, we show a set of spectroscopic line shapes taken over probe durations ranging from 40  $\mu\text{s}$  down to 2.6  $\mu\text{s}$ . Note that the fraction of atoms excited grows with decreasing resolution as our probe spectrum covers a larger fraction of the velocity distribution. For the shortest pulse length, the Fourier transform of the probe pulse has a spectral width approximately 2.2 times that of the Doppler distribution. As we see, changing the resolution from 21 kHz to 42 kHz (20  $\mu\text{s}$  pulse duration) begins to obscure the recoil splitting, but the large asymmetry persists.

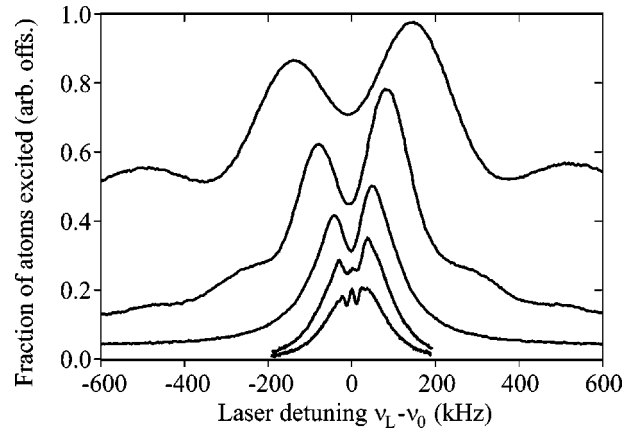


FIG. 4. Two-pulse spectra taken for probe pulse durations of 40, 20, 10, 6, and 2.6  $\mu\text{s}$  (bottom to top). Curves are vertically offset for clarity. The resolved recoil dips are clear in the smallest (highest resolution) curve (corresponding to Fig. 3), but are washed out for the lower resolutions while the recoil-induced asymmetry persists.

At a resolution of 85 kHz (10  $\mu\text{s}$  pulse duration), the recoil splitting is no longer visible as the two dips merge into a single saturated absorption dip centered at  $\nu_0$ , but the spectrum now appears to consist of two peaks whose separation is determined by the spectroscopic resolution and whose amplitudes differ by more than 25%. The asymmetry persists for even the lowest resolution, where the maxima are separated by 280 kHz, more than 10 times that of the recoil splitting itself.

Examination of Fig. 4 provides an intuitive picture of how such a small effect can cause such large asymmetries. In the Fourier-transform regime we find the spectroscopic condition where the widths of both the envelope and the dip are determined almost solely by the probe time, but are slightly offset from one another. This small offset leads to the envelope asymmetry because the dip intersects the Doppler envelope at different heights on the two sides. Thus the size of the asymmetry is related to the slope of the envelope multiplied by the size of the recoil effect.

## V. SIMPLE THEORETICAL MODEL

Alternatively, we can think of the saturated absorption spectrum as the sum of two contributions: one resulting from atoms that remain in the ground state after the first pulse and one resulting from atoms that were excited by the first pulse. This framework allows a simple model to describe our spectra well (an exact theoretical treatment of coherent saturation spectroscopy including multi-photon effects has been developed by Bordé and co-workers [9,12]). We start by considering the excitation spectrum resulting from the first (idealized) square  $\pi$  pulse of duration  $T$  and Rabi frequency  $\Omega$  illuminating a sample of ground-state atoms initially at rest. This yields the well-known Rabi spectrum [13] for the excitation probability:

$$P(\Delta) = \frac{\Omega^2 T^2}{4} \left( \frac{\sin[\sqrt{\Omega^2 + \Delta^2} T/2]}{\sqrt{\Omega^2 + \Delta^2} T/2} \right)^2, \quad (3)$$

where  $\Delta = \nu_L - \nu_A$  is the laser detuning from the absorption resonance (see Fig. 5). Illuminating the atoms with a square

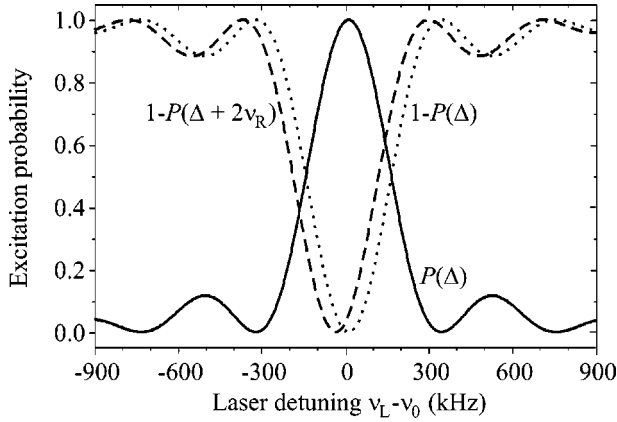


FIG. 5. Various theoretical excitation probabilities for a  $2.6 \mu\text{s}$  pulse for an atom initially at rest. The  $\text{sinc}^2$  spectra (see Eq. (3)) result from the square pulses in the time domain. The solid line is the excitation spectrum for an atom starting in the ground state while its inverse (dots) shows the probability for an atom to be left in the ground state after the first pulse. The shifted curve (dashed line) shows the probability for an atom to be left in the excited state by the second pulse.

$\pi$  pulse from the opposite direction gives two sets of atoms to consider. First, there are atoms that remain in the ground state after the first pulse [a fraction equal to  $1 - P(\Delta)$ ]; they will be resonant with a second pulse at frequency  $\nu_L = \nu_A$ , so the above equation applies to these atoms as well. Second, the atoms that were excited by the first pulse [a fraction equal to  $P(\Delta)$ ] now have a velocity  $v_r$  toward the second counterpropagating laser beam. The associated Doppler effect will shift the stimulated emission resonance down by one recoil, so these atoms will be resonant with light at frequency  $\nu'_{\text{SE}} = \nu_{\text{SE}} - \nu_r = \nu_0 - \frac{3}{2}\nu_r$  (i.e.,  $\nu'_{\text{SE}} = \nu_A - 2\nu_r$ ). The probability for these atoms to be left in the excited state can then be written as  $1 - P(\Delta + 2\nu_r)$ , using the same probability function  $P$  but with the argument shifted (see Fig. 5).

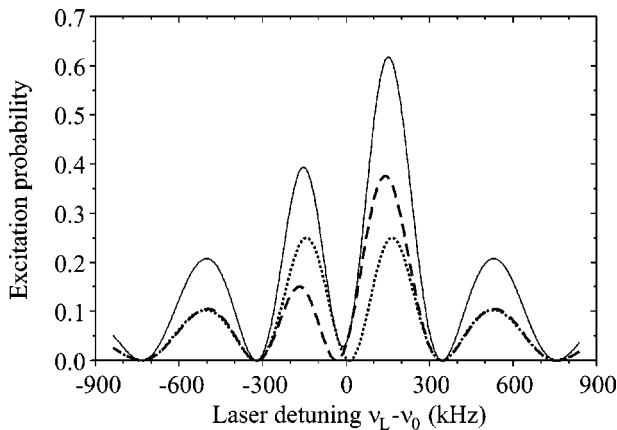


FIG. 6. The theoretical spectra resulting from products of the multiplicands shown in Fig. 5. The symmetric curve (dots) results from an atom still in the ground state after the first pulse, while the asymmetric component (dashed line) results from an excited state atom. The solid line is the sum of the two smaller curves and represents the saturated absorption spectrum for an atom at rest.

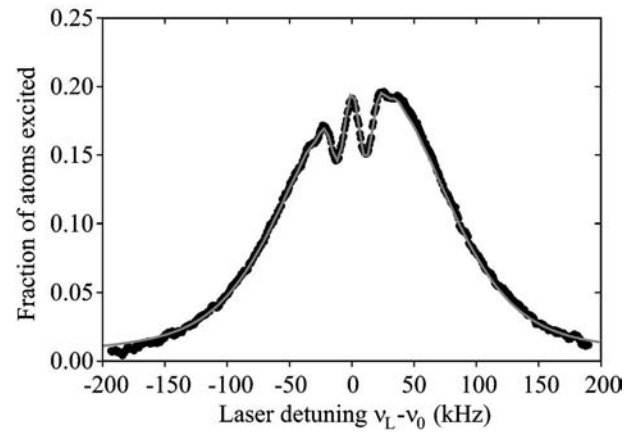


FIG. 7. Two-pulse spectrum (circles) resulting from probe pulses of  $40 \mu\text{s}$  duration (21 kHz resolution) along with the corresponding simulation (solid line).

To find the total fraction in the excited state after two pulses, we simply add the two contributions:

$$P_{\text{final}} = P(\Delta)[1 - P(\Delta)] + [1 - P(\Delta + 2\nu_r)]P(\Delta). \quad (4)$$

The first product in this expression gives the contribution of atoms still in the ground state after the first pulse and is symmetric about  $\nu_A$  (both pulses are resonant at the same frequency). The second term gives the contribution from atoms excited by the first pulse (and thus contains all stimulated emission effects), but it is asymmetric due to the offset of  $2\nu_r$  between arguments of the multiplicands. In Fig. 5 we have plotted the multiplicands for pulses of  $2.6 \mu\text{s}$  duration. In Fig. 6 we plot the products in Eq. (4) to show how they sum to yield a net asymmetric spectrum even for atoms initially at rest.

We can easily connect this model with experiment by summing over the initial velocity distribution (via the detuning) and the unequal laser intensities seen by the atoms due to the spatial distribution of the atoms in the laser mode (via the Rabi frequency). Note that the Doppler shift due to a nonzero initial velocity will have opposite signs for the two products in Eq. (4) since the two probe pulses come from opposite directions. The free parameters in our simulation were overall signal amplitude (imperfect normalization required a 10–15% reduction in signal size) and atomic cloud size (which we fixed at the same value for all simulations). We measured the velocity distributions and the laser mode size separately and used the resulting values for the simulations. We see good agreement over a variety of probe resolutions as shown in Figs. 7–9. At the high resolutions (Fig. 7), both model and experiment show additional smaller dips around the main dips that result from the wings of the  $\text{sinc}^2$  spectrum. Small differences in the wings between model and experiment at lower resolution (Fig. 9) most likely result from the nonideal square pulses used in the experiment.

Interestingly, we can isolate the second product in Eq. (4) for  $P_{\text{final}}$  experimentally by using recoil suppression [5,11]. In this case we remove the ground-state (symmetric) contribution by illuminating the atoms with a resonant 423 nm pulse (duration  $20 \mu\text{s}$ ) after the first red probe pulse but be-

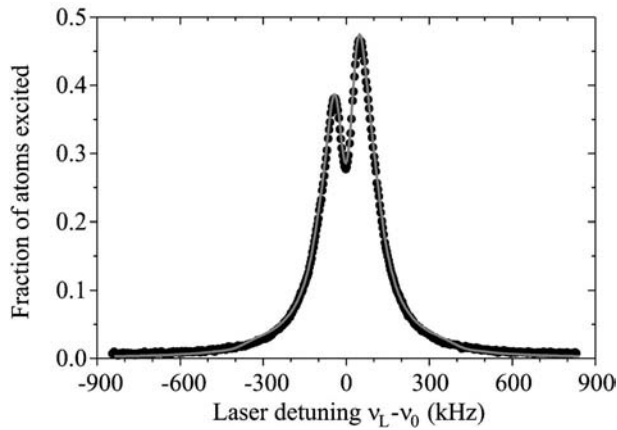


FIG. 8. Two-pulse spectrum (circles) resulting from probe pulses of  $10 \mu\text{s}$  duration (85 kHz resolution) along with the corresponding simulation (solid line).

fore the second red pulse. This heats the atoms in the ground state to the point where excitation by the second pulse produces a nearly flat Doppler background, underneath the signal from the atoms shelved in the excited state. Figure 10 shows the resulting spectrum taken with  $2.6 \mu\text{s}$  probe pulses; this Fourier transform-limited spectrum has larger asymmetry than that of Fig. 9, since the symmetric contribution has been suppressed. Comparison of the absolute peak heights shows that the feature associated with the excited state atoms is fully responsible for the spectral asymmetry in Fig. 9, as predicted by the simple model.

## VI. CONCLUSIONS

In summary, we have used ultracold two-level atoms to probe atomic recoil effects on saturated absorption spectroscopy at an unprecedented level. The resulting spectra clearly reveal the fundamental asymmetry in the location of recoil components on the Doppler background. In addition we have shown how this asymmetry in the recoil frequencies leads to large amplitude asymmetries in the Fourier transform limit, a

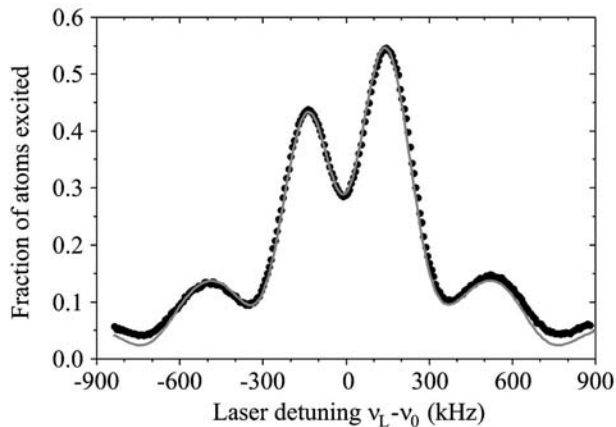


FIG. 9. Two-pulse spectrum (circles) resulting from probe pulses of  $2.6 \mu\text{s}$  duration (320 kHz resolution) along with the corresponding simulation (solid line).

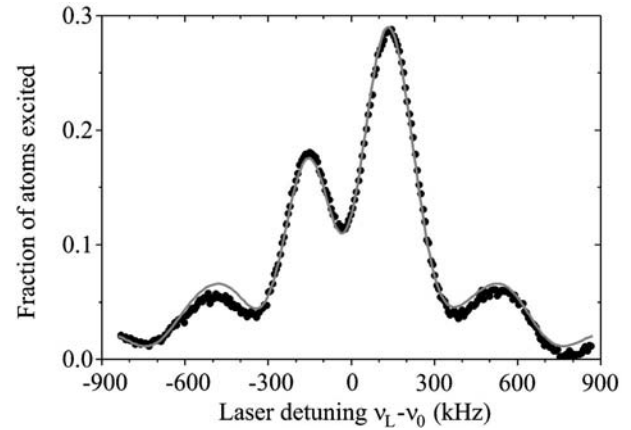


FIG. 10. Two-pulse saturated absorption spectrum (circles) for the excited state atoms resulting from probe pulses of  $2.6 \mu\text{s}$  duration along with the corresponding simulation (solid line). A resonant pulse at 423 nm with a duration of  $10 \mu\text{s}$  has been inserted between probe pulses to suppress the ground state component.

regime that has not previously been investigated but is important for state-of-the-art precision metrology. A simple model was developed that describes the spectra and observed asymmetries well.

We emphasize that these asymmetric envelopes persist in four-pulse Bordé-Ramsey saturation spectroscopy [12] in the Fourier transform regime, which is used in ultrahigh resolution studies and for neutral atom optical clocks [7,8]. To go from the two-pulse to the four-pulse case, each of the  $\pi$  pulses are divided into two  $\pi/2$  pulses separated in time. The use of short pulses enables all of the atoms to contribute coherently, thereby achieving high contrast signals. The resulting Ramsey-like high-resolution fringe patterns (see Fig. 11) have envelopes that are determined by their effective two-pulse spectrum, making them susceptible to the recoil asymmetries described in this paper. However, the good agreement between theory and experiments gives us confi-

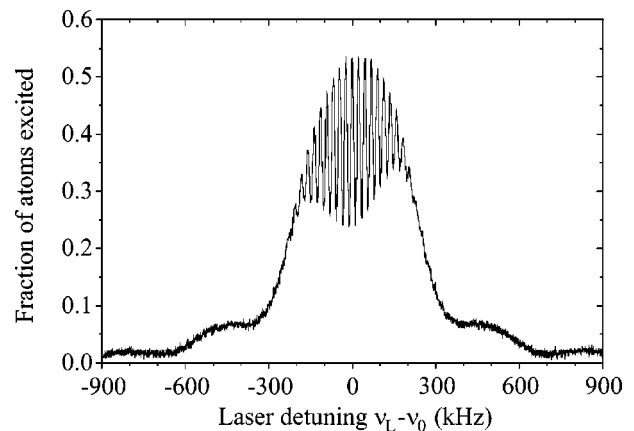


FIG. 11. Four-pulse Bordé-Ramsey spectrum resulting from  $3 \mu\text{s}$  probe pulses separated by  $21.6 \mu\text{s}$ . The Ramsey fringe structure (11.55 kHz resolution) has an asymmetric envelope that is directly related to the two-pulse spectra described in this paper.

dence that recoil-induced asymmetries will not limit the accuracy of these clocks. Extending these studies to a regime where Ca atoms are laser-cooled to subrecoil temperatures, as demonstrated by Curtis *et al.* [7], would allow individual addressing of the recoil components via laser detuning. This could enhance the sensitivity of precision measurements such as that of the photon recoil or other atom interferometry experiments [14–16].

#### ACKNOWLEDGMENTS

We thank J. Bergquist and J. Kitching for their insightful comments and J. L. Hall for illuminating discussions. This work was supported in part by NASA and ONR-MURI. G.W. acknowledges support from the Alexander von Humboldt Foundation. We also thank C. Wieman for the generous loan of a dye laser.

- 
- [1] A. P. Kol'chenko, S. G. Rautian, and R. I. Sokolovskiĭ, *Sov. Phys. JETP* **28**, 986 (1969).
  - [2] J. L. Hall, C. J. Bordé, and K. Uehara, *Phys. Rev. Lett.* **37**, 1339 (1976).
  - [3] R. L. Barger, J. C. Bergquist, T. C. English, and D. J. Glaze, *Appl. Phys. Lett.* **34**, 850 (1979).
  - [4] U. Sterr, K. Sengstock, J. H. Müller, D. Bettermann, and W. Ertmer, *Appl. Phys. B: Photophys. Laser Chem.* **B54**, 341 (1992).
  - [5] F. Riehle, J. Ishikawa, and J. Helmcke, *Phys. Rev. Lett.* **61**, 2092 (1988).
  - [6] S. N. Bagayev, A. E. Baklanov, V. P. Chebotayev, and A. S. Dychkov, *Appl. Phys. B: Photophys. Laser Chem.* **B48**, 31 (1989).
  - [7] E. A. Curtis, C. W. Oates, and L. Hollberg, *J. Opt. Soc. Am. B* **20**, 977 (2003).
  - [8] G. Wilpers, T. Binnewies, C. Degenhardt, U. Sterr, J. Helmcke, and F. Riehle, *Phys. Rev. Lett.* **89**, 230801 (2002).
  - [9] J. Ishikawa, F. Riehle, J. Helmcke, and C. J. Bordé, *Phys. Rev. A* **49**, 4794 (1994).
  - [10] T. Binnewies, G. Wilpers, U. Sterr, F. Riehle, J. Helmcke, T. E. Mehlstäubler, E. M. Rasel, and W. Ertmer, *Phys. Rev. Lett.* **87**, 123002 (2001).
  - [11] F. E. Dingler, V. Rieger, K. Sengstock, U. Sterr, and W. Ertmer, *Opt. Commun.* **110**, 99 (1994).
  - [12] C. J. Bordé, C. Salomon, S. Avrillier, A. Van Lerberghe, C. Bréant, D. Bassi, and G. Scoles, *Phys. Rev. A* **30**, 1836 (1984).
  - [13] I. I. Rabi, S. Millman, P. Kusch, and J. R. Zacharias, *Phys. Rev.* **55**, 526 (1939).
  - [14] D. S. Weiss, B. C. Young, and S. Chu, *Phys. Rev. Lett.* **70**, 2706 (1993).
  - [15] M. J. Snadden, J. M. McGuirk, P. Bouyer, K. G. Haritos, and M. A. Kasevich, *Phys. Rev. Lett.* **81**, 971 (1998).
  - [16] S. Gupta, K. Dieckmann, Z. Hadzibabic, and D. E. Pritchard, *Phys. Rev. Lett.* **89**, 140401 (2002).